AD-A060 830 WEAPONS RESEARCH ESTABLISHMENT SALISBURY (AUSTRALIA) F/G 20/6
COMPUTATION OF THE PERFORMANCE OF OPTICAL INTERFERENCE FILTERS --ETC(U)
MAR 78 M S BROWN

UNCLASSIFIED WRE-TR-1949(A) NL

1 OF 1
AD
A0 60830

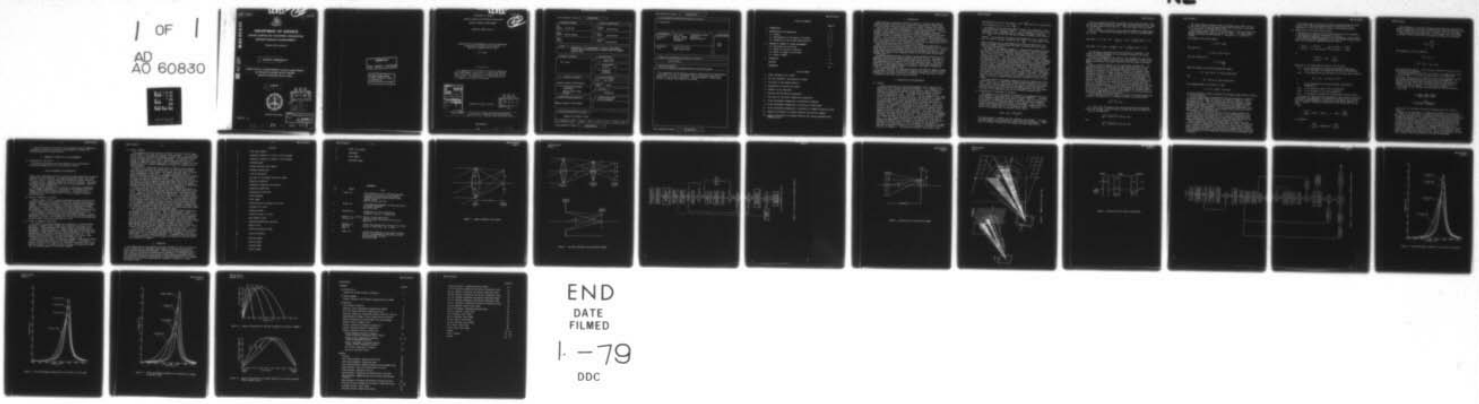

END
DATE FILMED
1-79
DDC

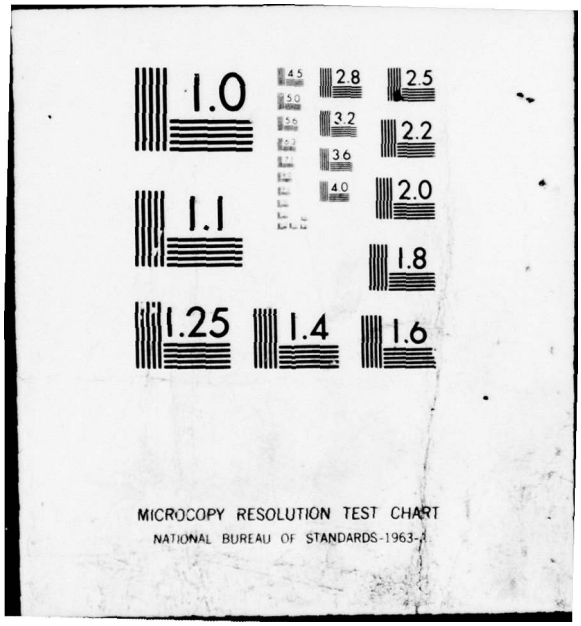
1.0
1.1
1.25
1.4
1.6
1.8
2.0
2.2
2.5
2.8
3.2
3.6
4.0
4.5
5.0
5.6
MICROCOPY RESOLUTION TEST CHART
NATIONAL BUREAU OF STANDARDS-1963-A

LEVEL II

(14) WRE-TR-1949(A)

AR-001-160

AD A060830

DDC FILE COPY

AUSTRALIA

DEPARTMENT OF DEFENCE

DEFENCE SCIENCE AND TECHNOLOGY ORGANISATION

WEAPONS RESEARCH ESTABLISHMENT

SALISBURY, SOUTH AUSTRALIA

(9) TECHNICAL REPORT, 1949 (A)

(6) COMPUTATION OF THE PERFORMANCE OF OPTICAL INTERFERENCE FILTERS USED IN FOCUSED OPTICAL SYSTEMS HAVING AN EXTENDED FIELD OF VIEW

(10) M.S. BROWN

(12) 31 p.

DEFENCE SCIENCE AND TECHNOLOGY ORGANISATION

Approved for Public Release

(11) MAR 1978

COPY No. 13

LEVEL

AR-001-160

DEPARTMENT OF DEFENCE

DEFENCE SCIENCE AND TECHNOLOGY ORGANISATION

WEAPONS RESEARCH ESTABLISHMENT

TECHNICAL REPORT 1949 (A)

COMPUTATION OF THE PERFORMANCE OF OPTICAL INTERFERENCE FILTERS USED IN FOCUSED OPTICAL SYSTEMS HAVING AN EXTENDED FIELD OF VIEW

M.S. Brown

SUMMARY

The computation of the effective spectral transmission of an interference filter when it is used in the focused beam of an optical system with an extended field of view is described. The performance of a Fabry-Perot filter in a typical lens system is discussed.

POSTAL ADDRESS: The Director, Weapons Research Establishment, Box 2151, G.P.O., Adelaide, South Australia, 5001.

DOCUMENT CONTROL DATA SHEET

Security classification of this page: UNCLASSIFIED

1 DOCUMENT NUMBERS	2 SECURITY CLASSIFICATION
AR Number: AR-001-160	a. Complete Document: Unclassified
Report Number: WRE-TR-1949(A)	b. Title in Isolation: Unclassified
Other Numbers:	c. Summary in Isolation: Unclassified

3 TITLE: COMPUTATION OF THE PERFORMANCE OF OPTICAL INTERFERENCE FILTERS USED IN FOCUSED OPTICAL SYSTEMS HAVING AN EXTENDED FIELD OF VIEW

4 PERSONAL AUTHOR(S):

M.S. Brown

5 DOCUMENT DATE: March 1978

6 6.1 TOTAL NUMBER OF PAGES: 28

6.2 NUMBER OF REFERENCES: 6

7 7.1 CORPORATE AUTHOR(S):

Weapons Research Establishment

7.2 DOCUMENT (WING) SERIES AND NUMBER

Applied Physics Wing TR-1949

8 REFERENCE NUMBERS

a. Task: DST 77/145

b. Sponsoring Agency: DSTO

9 COST CODE: 367020/115

10 IMPRINT (Publishing establishment):

Weapons Research Establishment

11 COMPUTER PROGRAM(S) (Title(s) and language(s))

12 RELEASE LIMITATIONS (of the document):

Approved for public release

12.0	OVERSEAS	NO		P.R.	1	A	2	B	1	C	1	D	1	E	1

Security classification of this page: UNCLASSIFIED

Security classification of this page: UNCLASSIFIED

13 ANNOUNCEMENT LIMITATIONS (of the information on these pages):

No limitation

14 DESCRIPTORS:

a. EJC Thesaurus Terms

Thin films
Interference filters
Optical filters
Radiometers
Optical lenses
Optical materials
Radiometry

b. Non-Thesaurus Terms

Optical thin films
Fabry-Perot filter

15 COSATI CODES:

2006
1402

16 LIBRARY LOCATION CODES (for libraries listed in the distribution):

SW SR SD AACA

17 SUMMARY OR ABSTRACT:
(if this is security classified, the announcement of this report will be similarly classified)

The computation of the effective spectral transmission of an interference filter when it is used in the focused beam of an optical system with an extended field of view is described. The performance of a Fabry-Perot filter in a typical lens system is discussed.

Security classification of this page: UNCLASSIFIED

TABLE OF CONTENTS

LIST OF FIGURES

1. INTRODUCTION

When multilayer interference filters are used in a conical light beam the effective spectral reflectance and transmission characteristics differ from those which apply when only parallel pencils at normal incidence are involved.

Some years ago a computer program(ref.1) was written to analyse the effect of conical light beams on the performance of narrow passband filters. In this program it was assumed that the filter was illuminated through a variable circular aperture for various conditions of filter orientation within the beam, so that the effect of different cone angles and filter tilt angles could be studied. This situation occurs when a filter is placed in the converging beam from a lens system which is focusing a point source object. The results obtained from this program can be used to determine the effect of cone angle and tilt on the location and spectral width of the filter passband.

When a multilayer filter is incorporated into an optical system with an extended field of view different sections of the object plane give rise to conical beams that are tilted at different angles to the surface of the filter. This is a more complicated situation than was considered previously and the filter performance will depend on the integrated effect of all the tilted conical beams incident upon it.

It recently became necessary to design a narrow passband filter for use in a radiometer system having a defined aperture and field of view. The spectral width and location of the filter passband when used in the lens system was of some importance and was required to lie within specified limits. In order to establish the design restrictions for the optical system, some additions and alterations to the computer program of reference 1 were made to include the effect of a defined field of view.

This report describes the modifications made to the previous computer program and discusses the effect of variations of aperture and field of view on the performance of all-dieletric Fabry-Perot interference filters when they are used in radiometers and other similar optical systems.

2. DESCRIPTION OF THE COMPUTATION

2.1 General

A brief discussion on the optical arrangement used in simple filter radiometers will illustrate the analysis problem. It is assumed in this analysis that the spectral radiance of the field of view is uniform or randomly distributed such that the average spectral radiance is uniform on a course macroscopic scale. The simplest use of a lens, filter, detector combination is shown in figure 1. The lens produces a real image of the field of view at the detector surface, and the filter is assumed to lie in any plane normal to the axis between the lens and the detector. The image formed is a faithful reproduction of a distant object and will contain the small intensity variations of the object field. This is undesirable in a radiometer because there may be variations in sensitivity across the detector. It is preferable to irradiate the detector surface uniformly and this is done in figure 2 by the use of a field lens which images the objective aperture onto the detector. The light entering the objective lens comes from all parts of the field of view and it is therefore uniformly illuminated across the aperture. The objective lens of aperture "A" produces an image of the object at the position occupied by the field lens. The focal length and position of the field lens is such that it produces an appropriately sized image of the aperture "A" at the detector. Although this optical system contains two lenses, for the purpose of analysing filter performance it can be considered as equivalent to a single lens with an aperture of diameter ($P \leqslant D$) located at a distance Q from the detector of diameter d. The important parameters which affect filter

performance are the half cone angle $a = \tan^{-1} \frac{(P/2)}{Q}$ and the tilt angle which has a maximum value of $t = \tan^{-1} (\frac{d/2}{Q})$.

The geometry of the equivalent optical system to be considered is that shown in the lower drawing of figure 2. At the centre of the detector the irradiation is by a convergent cone of light of half-angle a given by $\tan^{-1} \frac{(P/2)}{Q}$, with the axis of the cone at normal incidence to the detector surface. At the edge of the detector the irradiation is by a cone whose axis is tilted at an angle t given by $\tan^{-1} \frac{(d/2)}{Q}$. At other points on the detector surface there is some combination of the cone angle and a tilt angle, the former decreasing and the latter increasing with the distance from the detector centre.

The object of the computer program is to calculate the radiation falling on the detector (and also the filter) as a function of angle of incidence and hence to calculate the effective spectral transmission of the filter. This is done in two steps. Firstly, the detector surface is divided into annular rings centred on the axis of the optical system and having equal increments of radius. For each ring a mean cone and tilt angle is computed for the geometry of the lens system under consideration. Having established the mean cone and tilt angle associated with each ring the original program (ref.1) is used to determine the distribution of the radiation over the incidence angles contained within each tilted cone. This population is given a weighting factor proportional to the area of the ring on the detector surface with which the cone is associated. The analysis is performed for each ring in turn from the centre of the detector to the edge. The angular distribution of radiation for all rings is summed so that the final output from the first part of the program is an array of angles and the relative amount of radiation incident on the detector, and also the filter, at those angles.

The second half of the program computes the spectral transmission of the interference filter at each of the incidence angles specified by the first half. These spectral transmission curves are then weighted by the angular distribution of the incident radiation and summed to give the effective spectral transmission curve of the filter when operated in the lens system. The steps in the computation will now be discussed in greater detail.

2.2 Determination of the angles of incidence

The geometry of the lens system is defined for the program by the equivalent aperture P, the separation Q and the detector diameter d. Referring to the computer program flow chart shown in figure 3 the first step in the calculation is to determine the angles at which the spectral performance of the filter will be calculated later in the program. This is done by computing the maximum angle of incidence of the light falling on the filter surface and dividing this into ten incremental angles. Referring to figure 2 the maximum angle of incidence of the cone is:

$$\theta \text{ max} = \tan^{-1} (\frac{d/2 + P/2}{Q})$$

The minimum angle is normally zero for concentric lens systems. Ten angles have been found to give satisfactory results from the calculations. Using smaller increments of angle does not change the result significantly.

The next program step divides the detector surface into concentric rings and calculates the cone and tilt angles which are associated with each ring. Let the mean radius of the ring be r. Then from figure 4 the tilt angle $t = \tan^{-1}(r/Q)$.

The cone angle is obtained by calculating the maximum and minimum angles in the cone. Then the half cone angle, which is half the included angle $(\delta - \eta)$ is:

$$\text{cone angle} = 0.5 \left(90 + \tan^{-1}\left(\frac{P/2 - r}{Q}\right) - \tan^{-1}\left(\frac{Q}{r + P/2}\right) \right) \text{ when } r < P/2$$

$$\text{cone angle} = 0.5 \left(\tan^{-1}\left(\frac{Q}{r - P/2}\right) - \tan^{-1}\left(\frac{Q}{r + P/2}\right) \right) \text{ when } r > P/2$$

The remaining calculations were fully described in reference 1, but because of changes introduced in the notation an account of the steps involved will be given here.

The angle of incidence at the filter is then evaluated for rays from a number of regularly spaced locations within the aperture to establish the angular distribution of incident radiation within the range of incidence angles.

Figure 5 shows the geometry of the system under consideration. The upper diagram shows a conical beam of light emanating from a circular aperture of radius D/2 in a plane perpendicular to the cone axis and focusing at the point 0 on the filter. One half of the plane is shown divided into an array of squares located at positions specified by the coordinate system, x,y. When considering the case for that portion of the filter at normal incidence to the axis of the irradiating cone, the aperture is assumed to be in the plane as shown in the top diagram. To consider those parts of the filter tilted to the axis of the irradiating cone it is assumed that the aperture and filter are rotated about the x-axis by the angle of tilt. The top half of the aperture will then lie behind the plane containing the grid reference x,y and the lower half will lie in front of it. To establish the distribution of incidence angles for rays passing through all parts of the aperture the incidence angle is calculated at each position on the aperture where it is cut by lines from the origin through the grid positions x,y.

All the squares in the array which lie within the circular aperture are included in the analysis i.e. at normal incidence all positions where

$$\sqrt{x^2 + y^2} \leq P/2$$

For tilted cones (the general case) the grid positions are projected back to the vertical to test if they lie within the circle of radius P/2.

They are included when:

$$\sqrt{x^2 + (y.\cos t)^2} \leq P/2 \text{ for +VE } y$$

and

$$\sqrt{x^2 + (y/\cos t)^2} \leq P/2 \text{ for -VE } y$$

The lower diagram on figure 5 shows an enlarged view of ABCD a portion of the surface of the grid reference plane with the aperture tilted about the x-axis, which is the most general case.

The incidence angle θ which is to be calculated is the angle between the incident light and the normal at the filter surface. For light passing through the aperture at the position C', the angle θ is calculated as follows:

From figure 5 the vertical angle:

$$\beta = \tan^{-1} (y/OA)$$

The angle ψ is:

$$\psi = \tan^{-1} (x/(OA \sec \beta))$$

From the triangle OC'F'

$$\theta = \cos^{-1} \frac{OF'}{OC'}$$

Where the normal to the filter and aperture planes

$$OF' = OB' \cos (\beta + t) \text{ from triangle } OB'F'$$

and

$$OC' = OB' . \sec \psi \text{ from triangle } OB'C'$$

The incidence angle on the filter is then:

$$\theta = \cos^{-1} (\cos(\beta + t)\cos (\psi))$$

A similar procedure is used to calculate the incidence angle from the position (x,-y) below the axis.

As the incidence angle associated with each grid position is evaluated, the nearest assigned angle is found and an integer is added to a store associated with it. When the aperture area has been completely scanned, the population held in the store associated with each assigned incidence angle gives the number of grid positions where this assigned value of incidence angle was encountered. For the calculations discussed in this paper, x and y were arbitrarily given maximum values of ±50 (i.e. 2500 π unit squares in the irradiated area).

This analysis is carried out for cone and tilt angles specified for each of the rings on the filter surface. The total population at each assigned angle after the completion of this analysis is multiplied by a factor proportional to the area of each ring, and normalised to give the angular distribution of the irradiance incident on the filter.

Having established a range of incidence angles and their associated relative intensity figures for light incident on the filter, the next step is to calculate the performance of the filter at each of these incidence angles, multiply the values of the reflection or transmission coefficient by the angular distribution, and sum the ten performance curves to give the integrated effect for the irradiation conditions over the wavelength range of interest.

The methods used to calculate the reflection and transmission coefficients of the filter were described fully in reference 2, but for completeness a brief description is given in the following section.

2.3 Computation of the filter characteristics

The method of calculation and the notation used are those suggested by Weinstein(ref.3) and are illustrated in figure 6.

The tangential components of the electric and magnetic field strength vectors E(J+1) and H(J+1) immediately to the left of the Jth layer of the thin film system may be expressed in matrix from as:

$$\begin{pmatrix} E(J+1) \\ H(J+1) \end{pmatrix} = \begin{pmatrix} \cos g(J) & \frac{i}{u(J)} \sin g(J) \\ i\, u(J) \sin g(J) & \cos g(J) \end{pmatrix} \cdot \begin{pmatrix} E(J) \\ H(J) \end{pmatrix}$$

or

$$\begin{pmatrix} E(J+1) \\ H(J+1) \end{pmatrix} = M(J) \cdot \begin{pmatrix} E(J) \\ H(J) \end{pmatrix}$$

Where M(J) is the characteristic matrix of the Jth layer.

- u(J) may be considered as an effective refractive index which varies with angle of incidence and the state of polarisation
- g(J) is the effective optical thickness of the layer, and is given by:

$$g(J) = 2\pi/\lambda \cdot n(J)\, h(J) \cos \theta(J)$$

- λ is the wavelength of the radiation under consideration (nanometres)
- n(J) is the refractive index of the layer material
- h(J) is the thickness of the layer (nanometres)
- $\theta(J)$ is the angle of incidence of the radiation in the Jth layer

By successively applying this relationship to each layer of a thin film construction, an expression is obtained for the values of E(P) and H(P), the field strength immediately to the left of the outside layer of the filter, (figure 6) in terms of the matrices of the layers and E(1) and H(1).

Thus

$$\begin{pmatrix} E(\rho) \\ H(\rho) \end{pmatrix} = M(\rho-1) \cdot M(\rho-2) \cdots\cdots M(1) \cdot \begin{pmatrix} E(1) \\ H(1) \end{pmatrix}$$

or in general

$$\begin{pmatrix} E(\rho) \\ H(\rho) \end{pmatrix} = M(\text{product}) \cdot \begin{pmatrix} E(1) \\ H(1) \end{pmatrix}$$

Where M(product) is the matrix formed by multiplying the characteristic matrix of each layer by the next succeeding layer matrix and continuing the process through the filter from layer 1 to layer $(\rho-1)$, the final layer.

Having calculated the product matrix of the complete thin film system, the values of $E(\rho)$ and $H(\rho)$ may be calculated by using the relationship

$$n_{(J)} = \frac{H_{(J)}}{E_{(J)}}$$

and assuming the initial conditions

$$E(1) = E_{(s)} = 1$$

$$H(1) = n_{(s)} \cdot E_{(s)} = n_{(s)}$$

and evaluating the matrix. (The subscript s denotes the value of E and n pertaining to the substrate.)

If absorbing materials are used in the filter, the complex form of the refractive index $n = N - iK$ must be used, where K is the absorption coefficient, which leads to a reduction of the complex amplitude by $e^{-2\pi K}$ per vacuum wavelength traversed in the direction of propagation. The complex refractive index may be substituted directly into the above equations instead of n(J), and the values of $E(\rho)$ and $H(\rho)$ which are produced will then be complex. See for instance reference 4.

The reflection and transmission coefficients may then be calculated (ref.5) from:

$$R = \left| \frac{E(\rho) - H(\rho) / N(\rho)}{E(\rho) + H(\rho) / N(\rho)} \right|^2$$

$$T = \frac{4N_{(s)}}{N(\rho) \left| E(\rho) + H(\rho)/N(\rho) \right|}^2$$

A flow chart for the matrix calculation and graph plotting is shown in figure 7.

Because of the large number of computations performed by the program in any single run, output from it is normally restricted to the final graph showing the effective spectral transmission of the filter under the specified illumination conditions. The optical constants of the materials used in the thin film designs under analysis are read from a data set (described in reference 6) which contains a library of the optical constants of the substrate and evaporation materials used in the manufacture of thin film interference filters. The library is updated when new materials are used or the evaporation conditions are changed, as these effect the optical constants of materials in thin film form. The filter description, wavelength and plotting specifications and the optical system geometry are read from a separate data set allocated by the controlling program.

As an illustration of the type of result obtained from the computation two examples of narrow passband filter performance in focused lens systems are given in the next section.

3. EXAMPLES OF CHANGES IN FILTER PERFORMANCE

3.1 Description of the filter

The filter construction under consideration is an all-dielectric Fabry-Perot design which has a layer system as follows:

substrate/HLHLHLHL.12H.LHLHLHLH/air

where H and L represent high and low refractive index layers with an optical thickness of $\lambda/4$ at 1060 nm. At normal incidence the filter has a half width (T = 50%) of 1.3 nm and when the substrate back surface reflection is omitted it has a computed transmission of 96.6% at 1060 nm. The normal incidence spectral transmission curve for the filter passband is shown as the highest curve in figure 10.

The two cases considered in this section are variation of performance due to changes in aperture (i.e. variations in the F-number) and due to changes in field angle (diameter of detector). The filter can be considered to lie in any plane normal to the axis between the aperture and the detector.

3.2 Effect of variation of aperture

Figure 8 shows a series of spectral transmission curves for the filter when the aperture of an irradiation system with a constant field angle is changed. The dimensions chosen are a variable aperture of 20 mm maximum diameter, a fixed detector diameter of 10 mm and a separation of 80 mm, giving an F/4 system at full aperture and a semi-field angle of 3.58^{o} at full aperture. Under these conditions, the filter peak transmission drops to 52% and shifts to 1059 nm, and the half width increases to 3.0 nm.

As the aperture is decreased the filter performance improves. At an aperture of 10 mm (F/8) the transmission rises to 76% at 1059.6 nm and the half width is 1.9 nm. At an aperture of 5 mm (F/16) the peak transmission is 87% at 1059.7 nm and the half width is 1.7 nm.

3.3 Effect of change in field angle

The effect of field angle changes was calculated for a 10 mm diameter aperture, a variable filter diameter and a separation of 80 mm i.e. an F/8 system. These parameters were chosen to give a reasonable filter performance as shown by figure 8. Figure 9 shows that in the worst case considered, a 20 mm diameter detector (semi-field angle of 7.12^{o}) the peak transmission is 55% at 1059.2 nm and the half width is 2.9 nm. The smallest detector diameter, 5 mm (semi-field angle 1.79^{o}) gives a peak transmission of 85% at 1059.7 nm and a half width of 1.5 nm.

Figure 10 shows the effect of varying the F-number of the optical system when the aperture and detector are the same diameter. The trends are similar to those shown in figure 7 for variations in aperture with a fixed detector diameter. Providing the filter is used at an aperture no wider than F/8 the performance is not markedly degraded.

3.4 General comments

The parameters which were varied in Section 3.2 and 3.3 have the same general effect on the shape and location of the passband. As the aperture of the system is increased the bandwidth increases, the transmission drops and the passband shifts to a shorter wavelength. The reason for these changes is simply that the filter is being irradiated with light at a variety of different incident angles and, as predicted by theory the filter passband shifts to a shorter wavelength as the angle of incidence of the light increases.

Several of the transmission curves shown on figures 8 and 9 represent cases where the aperture size and detector size have been interchanged. From consideration of the relevant ray diagrams one would expect a similar filter performance in these cases. The small differences that are apparent between the curves for interchanged dimensions are due to rounding errors in the numerical integration process. Taking smaller increments of angles and radii on the detector surface would reduce these errors at the expense of greater computer storage requirements during the calculation. These errors are smaller than the differences which often occur between computed and measured filter performance due to inaccuracies of manufacture and errors in the refractive indices used in the computations.

For the particular case of figure 8 the angular energy distribution of the incident radiation has been plotted for each of the transmission curves shown. Figure 11 shows the normalised angular energy distribution which is the output from the first half of the computation. The characteristic shape of the distribution is the same in each case, but the angular spread increases with the aperture of the lens system. For the smallest aperture the transmission peaks calculated at each of the incidence angles shown in curve A (figure 11) overlap to produce a narrow, high transmission region. As the aperture is increased the range of incidence angles is greater and the effective transmission peaks are spread over a greater wavelength range. The resultant passband is then wider and lower in transmission because there is less overlap in the individual transmission peaks.

The energy distribution over the range of incidence angles changes with the geometry of the optical system. This is demonstrated in figure 12 which shows the output from the first part of the computation for a variety of different ratios of aperture to detector diameter at a fixed separation. The curves have been normalised to remove the effect of different detector diameters and they are plotted against a normalised range of incidence angles. When the aperture and detector diameters are equal the distribution is approximately symmetrical over the range of angles as shown by curve A. When the aperture and detector diameters are different there is more energy incident at higher angles of incidence as shown by curves B and C.

If a filter is to be used under these irradiation conditions it would be necessary to make it at a longer wavelength than required so that the wavelength shift of the transmission peak due to the convergence of the lens system moves it to the correct wavelength. A compromise would be necessary if a variable aperture is involved because the location of the peak shifts as the aperture is changed.

4. CONCLUSION

This computation has been applied to filters intended for use in a variety of optical systems and has provided a useful method of assessing the effective filter passband location and bandwidth. The results of the computation have been useful in specifying the optimum control wavelength for the manufacture of narrow passband filters for use in optical systems having an extended field of view over which the spectral radiance can be considered uniform or to be randomly distributed such that the average spectral radiance is uniform on a course macroscopic scale.

NOTATION

D	field lens diameter
E	tangential component of electric field strength
H	tangential component of magnetic field strength
I	incidence angle
J	integer denoting layer numbers
K	absorption coefficient
M	a two by two matrix
N	real part of the complex refractive index
P	diameter of aperture
Q	separation of aperture and detector
R	reflection coefficient
T	transmission coefficient
d	filter diameter
f	focal length
g	effective optical thickness of a layer
h	thickness of a layer
i	complex constant
n	refractive index of a layer
r	mean radius of ring
s	subscript denoting the substrate
t	angle of tilt
u	effective refractive index
x, y	array co-ordinates
α	half cone angle
β	vertical angle
δ	vertical angle
η	vertical angle

θ	angle of incidence
λ	wavelength
ρ	layer number
ψ	horizontal angle

REFERENCES

No.	Author	Title
1	Brown, M.S.	"The Influence of Tilt, Cone Angle and Beam Intensity Cross-Section on the Computed Performance of Narrow Band Optical Interference Filters" WRE-TN-710(AP), July 1972
2	Brown, M.S.	"The Computed Performance of Thin Film Filters at Oblique Incidence" WRE-TN-571 (AP)
3	Weinstein, W.	"Computations in Thin Film Optics" Vacuum Vol. IV, No. 1, January 1954
4	Nestell, J.E. Jnr and Christy, R.W.	"Optics of Thin Metal Films" American Journal of Physics Vol.39, p.313, March 1971
5	Berning, P.H. Edited by HASS, G.	"Theory and Calculations of Optical Thin Films" Physics of Thin Films, Vol. 1, 1963
6	Brown, M.S.	"Interactive Computing of the Normal Incidence Spectral Transmission and Reflection of Thin Film Interference Filters" WRE-TM-1615 (AP)

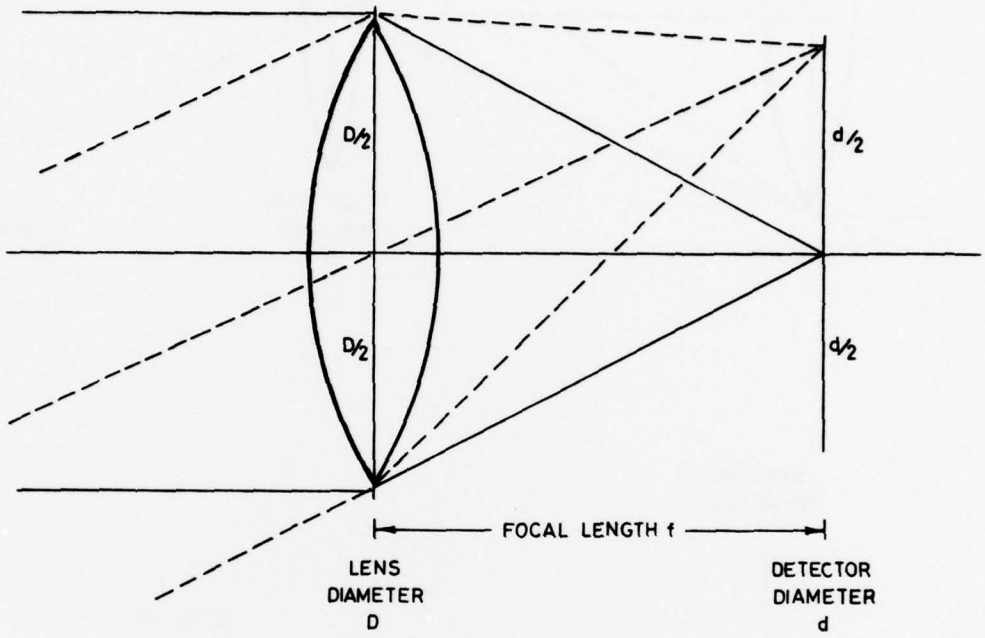

Figure 1. Simple radiometer lens system

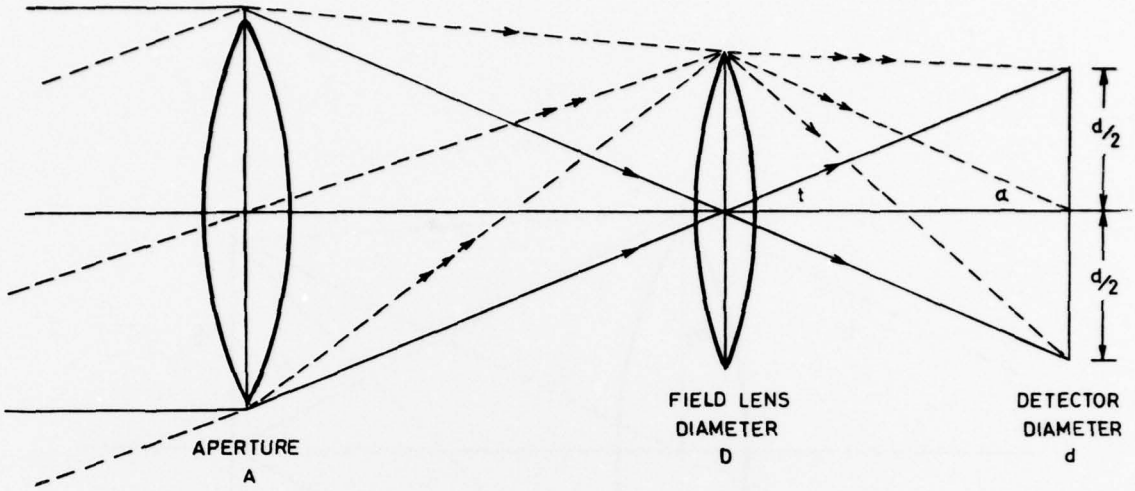

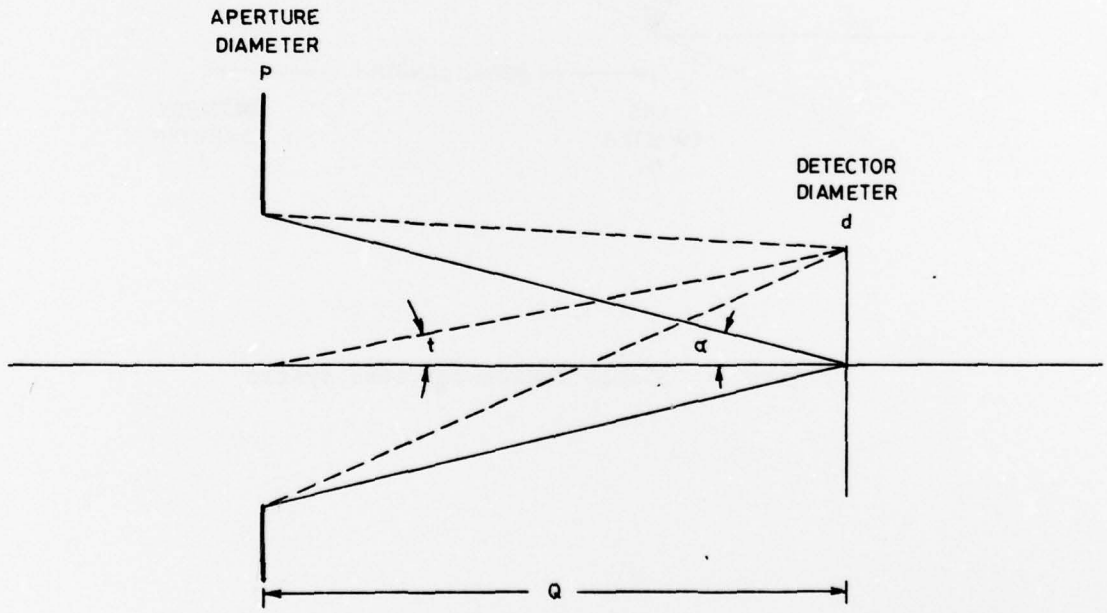

Figure 2. Two lens radiometer and equivalent diagram

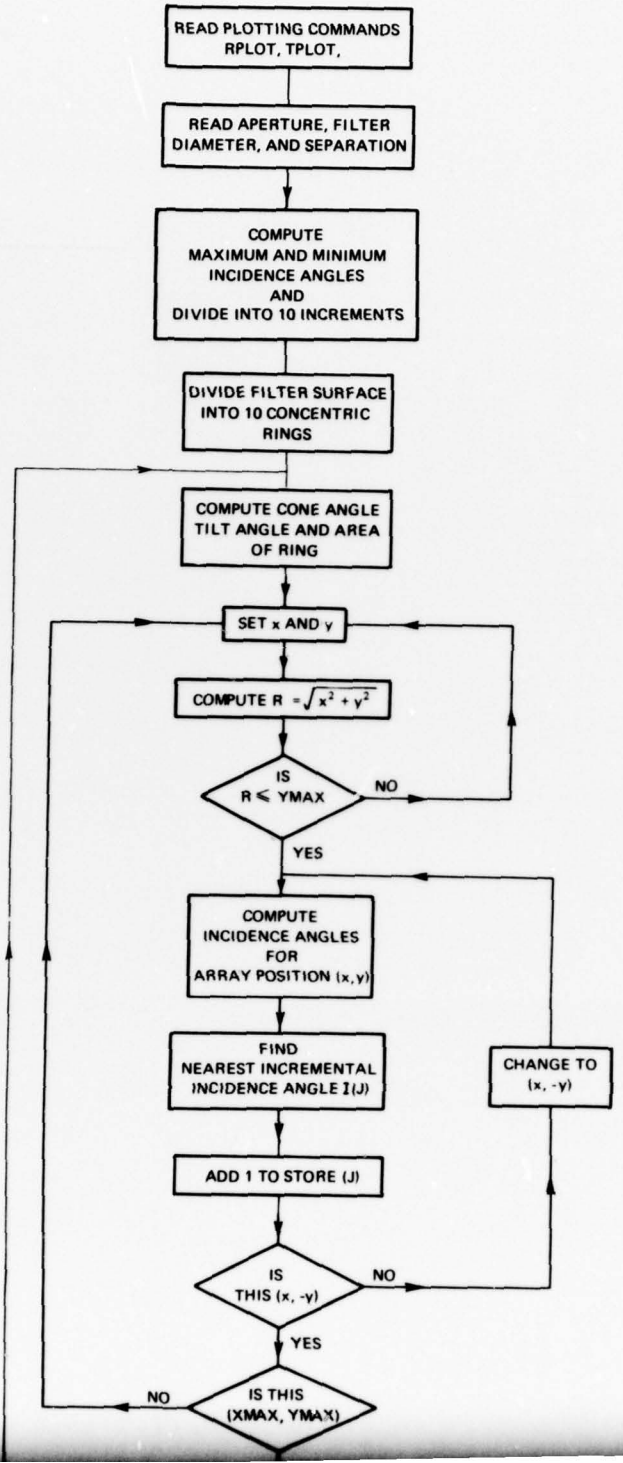
READ PLOTTING COMMANDS RPLOT, TPLOT,
READ APERTURE, FILTER DIAMETER, AND SEPARATION
COMPUTE MAXIMUM AND MINIMUM INCIDENCE ANGLES AND DIVIDE INTO 10 INCREMENTS
DIVIDE FILTER SURFACE INTO 10 CONCENTRIC RINGS
COMPUTE CONE ANGLE TILT ANGLE AND AREA OF RING
SET x AND y
COMPUTE R = $\sqrt{x^2 + y^2}$
IS R ≤ YMAX
NO
YES
COMPUTE INCIDENCE ANGLES FOR ARRAY POSITION (x,y)
FIND NEAREST INCREMENTAL INCIDENCE ANGLE I(J)
CHANGE TO (x, -y)
ADD 1 TO STORE (J)
IS THIS (x, -y)
NO
YES
NO
IS THIS (XMAX, YMAX)

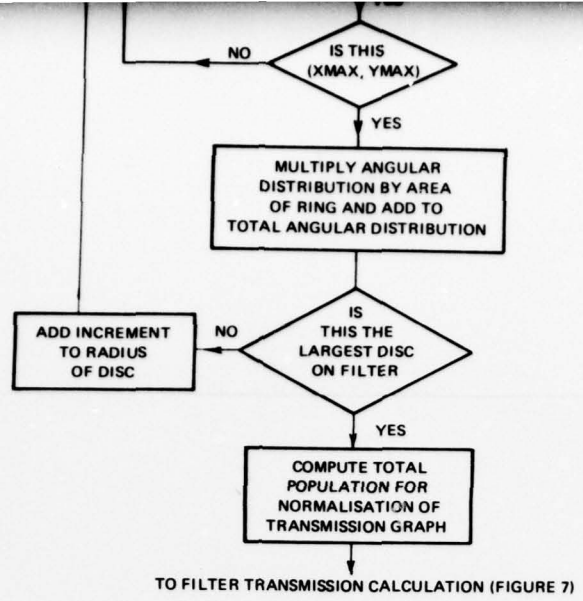

Figure 3. Flow chart of the angular analysis

Figure 3

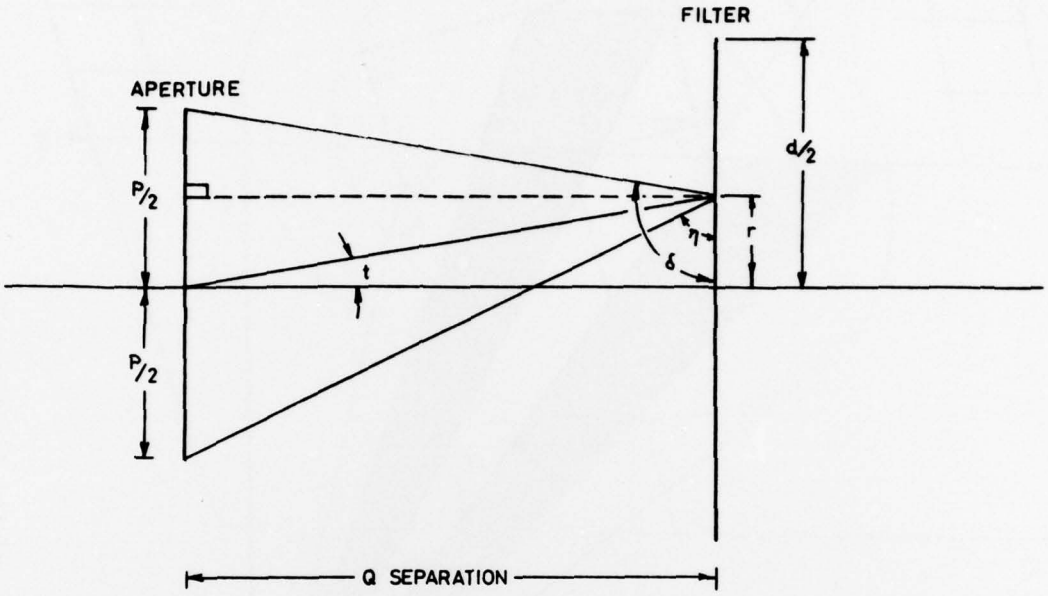

Figure 4. Calculation of cone and tilt angles

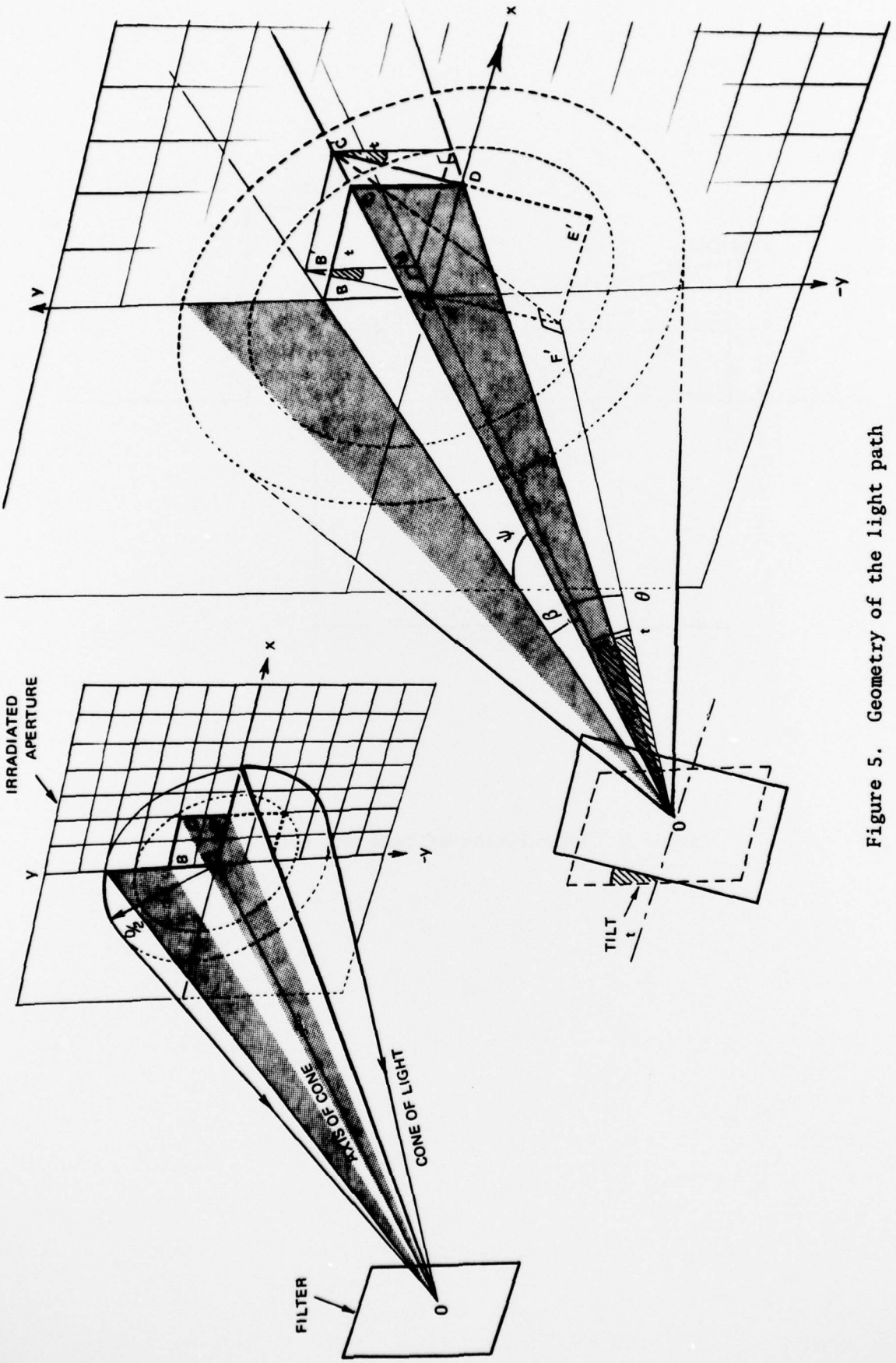

Figure 5. Geometry of the light path

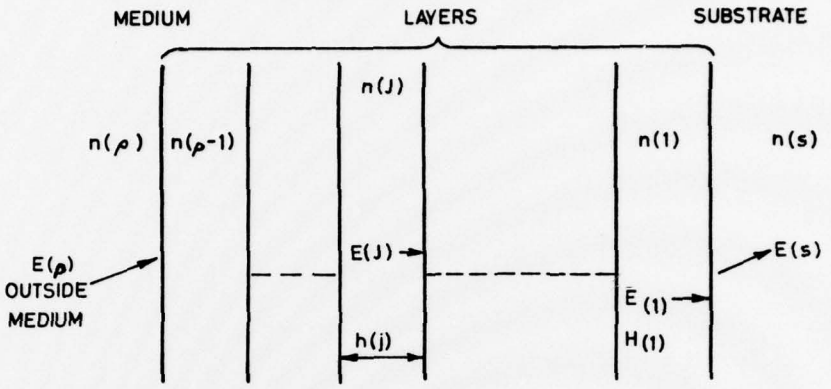

Figure 6. Notation used for matrix calculations

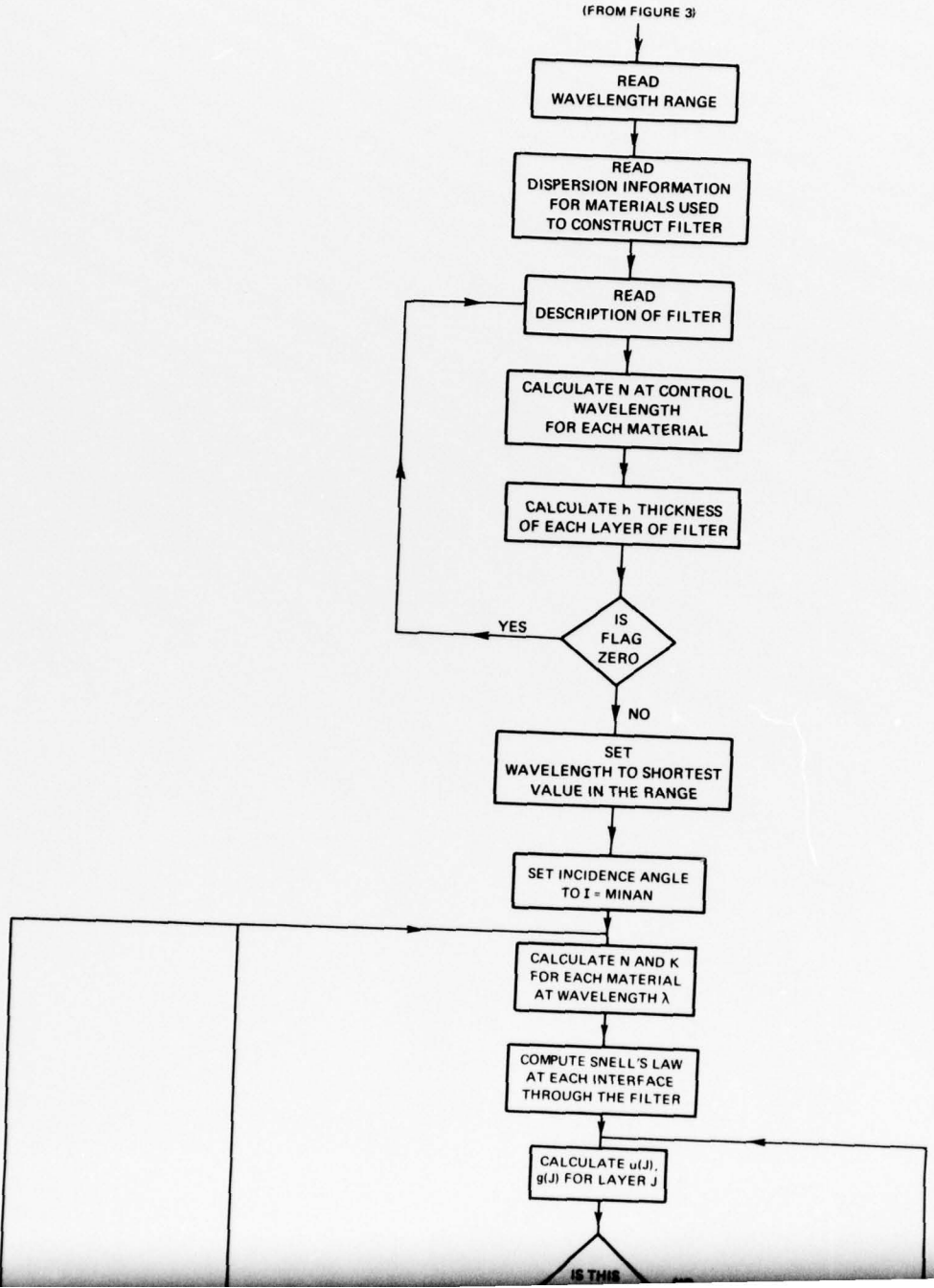
(FROM FIGURE 3)
READ WAVELENGTH RANGE
READ DISPERSION INFORMATION FOR MATERIALS USED TO CONSTRUCT FILTER
READ DESCRIPTION OF FILTER
CALCULATE N AT CONTROL WAVELENGTH FOR EACH MATERIAL
CALCULATE h THICKNESS OF EACH LAYER OF FILTER
IS FLAG ZERO
YES
NO
SET WAVELENGTH TO SHORTEST VALUE IN THE RANGE
SET INCIDENCE ANGLE TO I = MINAN
CALCULATE N AND K FOR EACH MATERIAL AT WAVELENGTH λ
COMPUTE SNELL'S LAW AT EACH INTERFACE THROUGH THE FILTER
CALCULATE u(J), g(J) FOR LAYER J
IS THIS

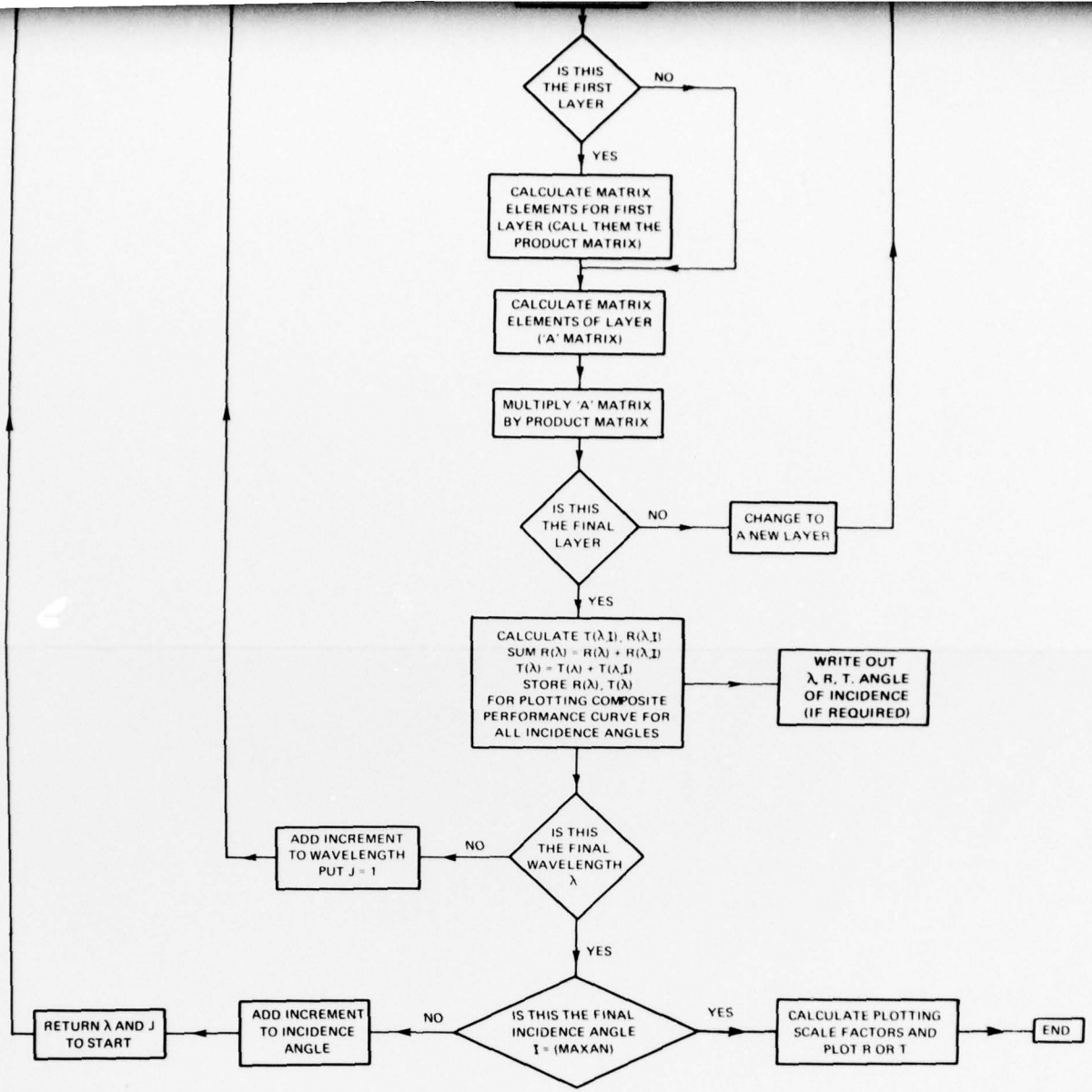

Figure 7. Flow chart of the filter transmission calculation

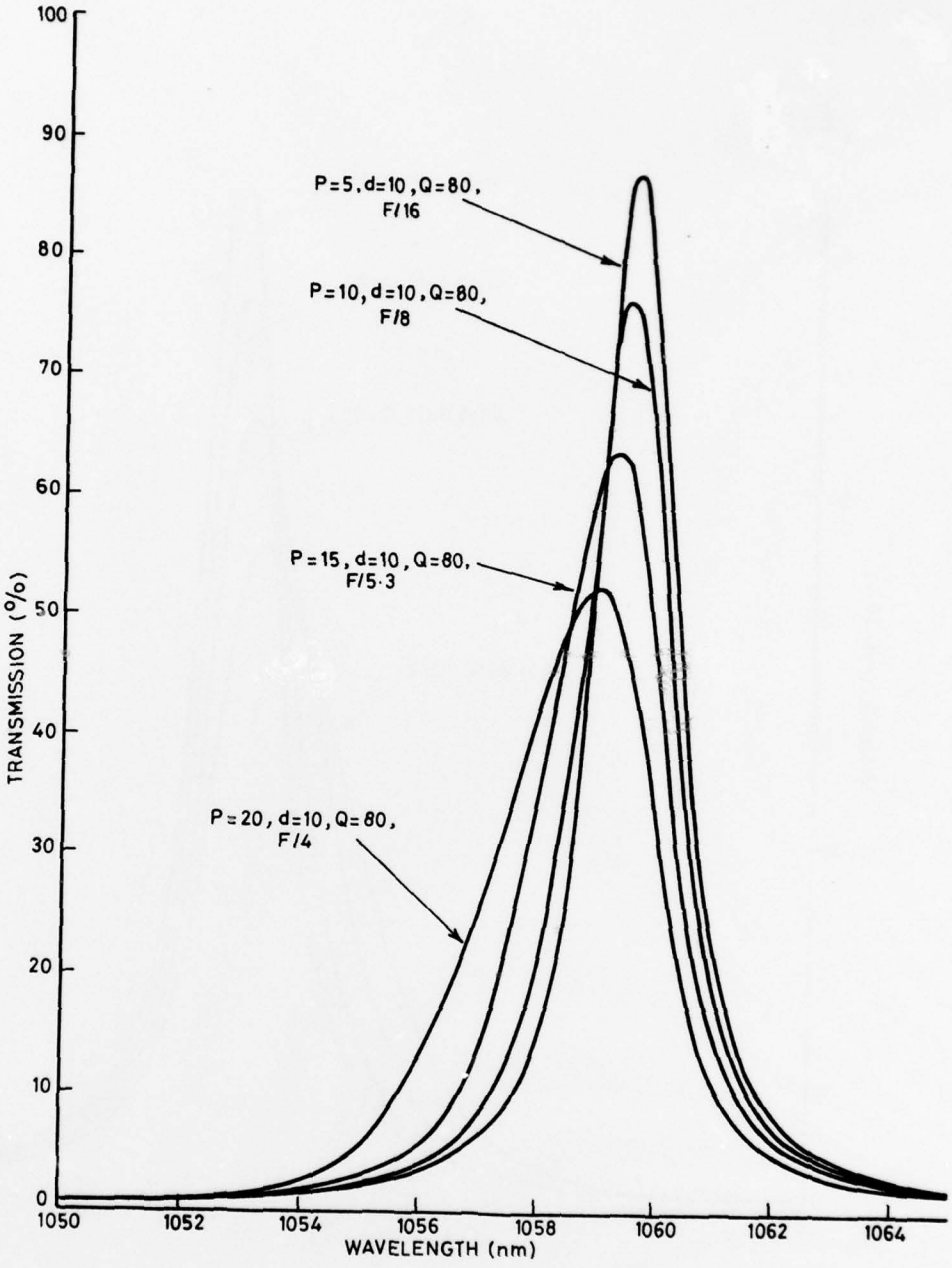

Figure 8. Filter performance changes due to variations in aperture

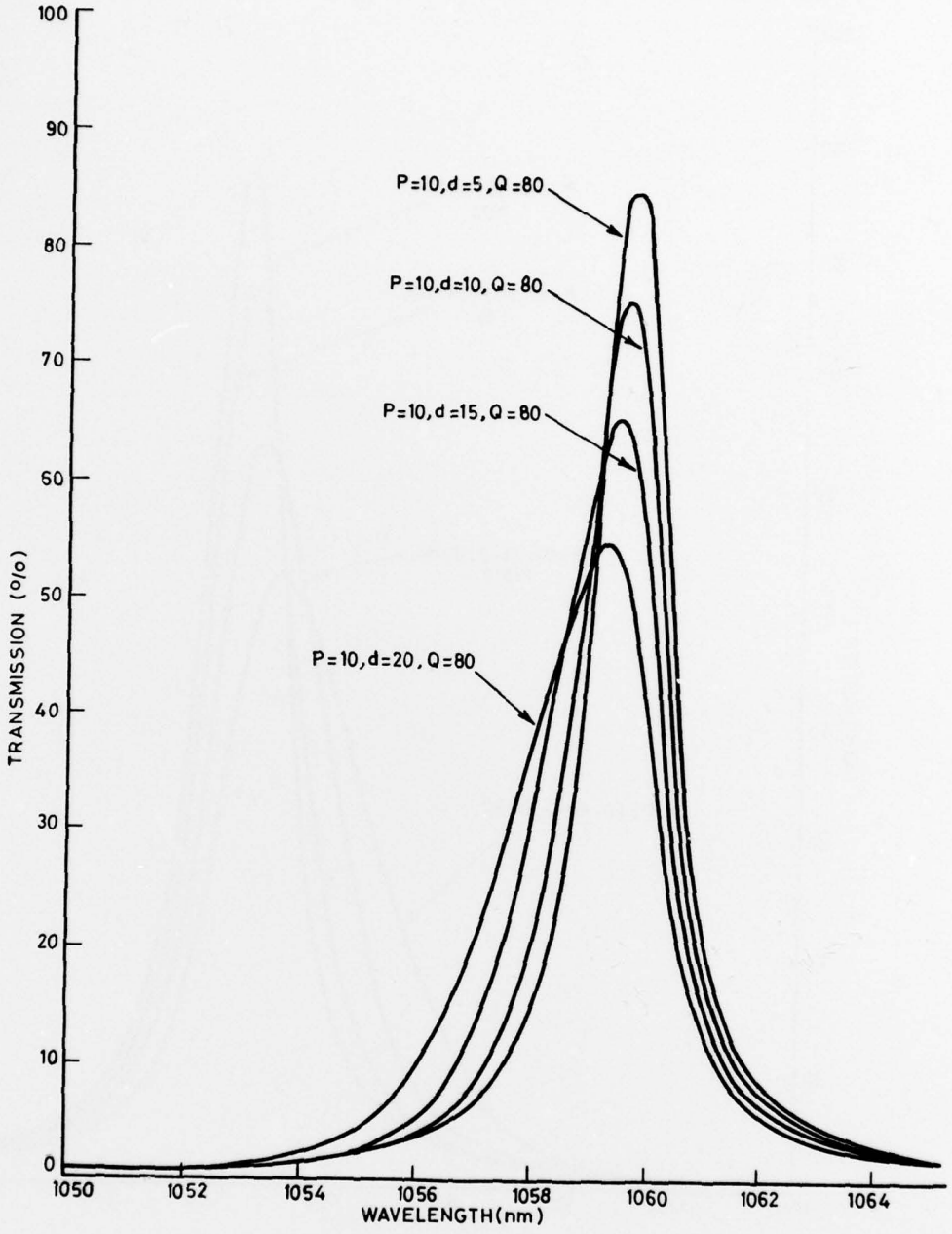

Figure 9. Filter performance changes due to variations in field angle

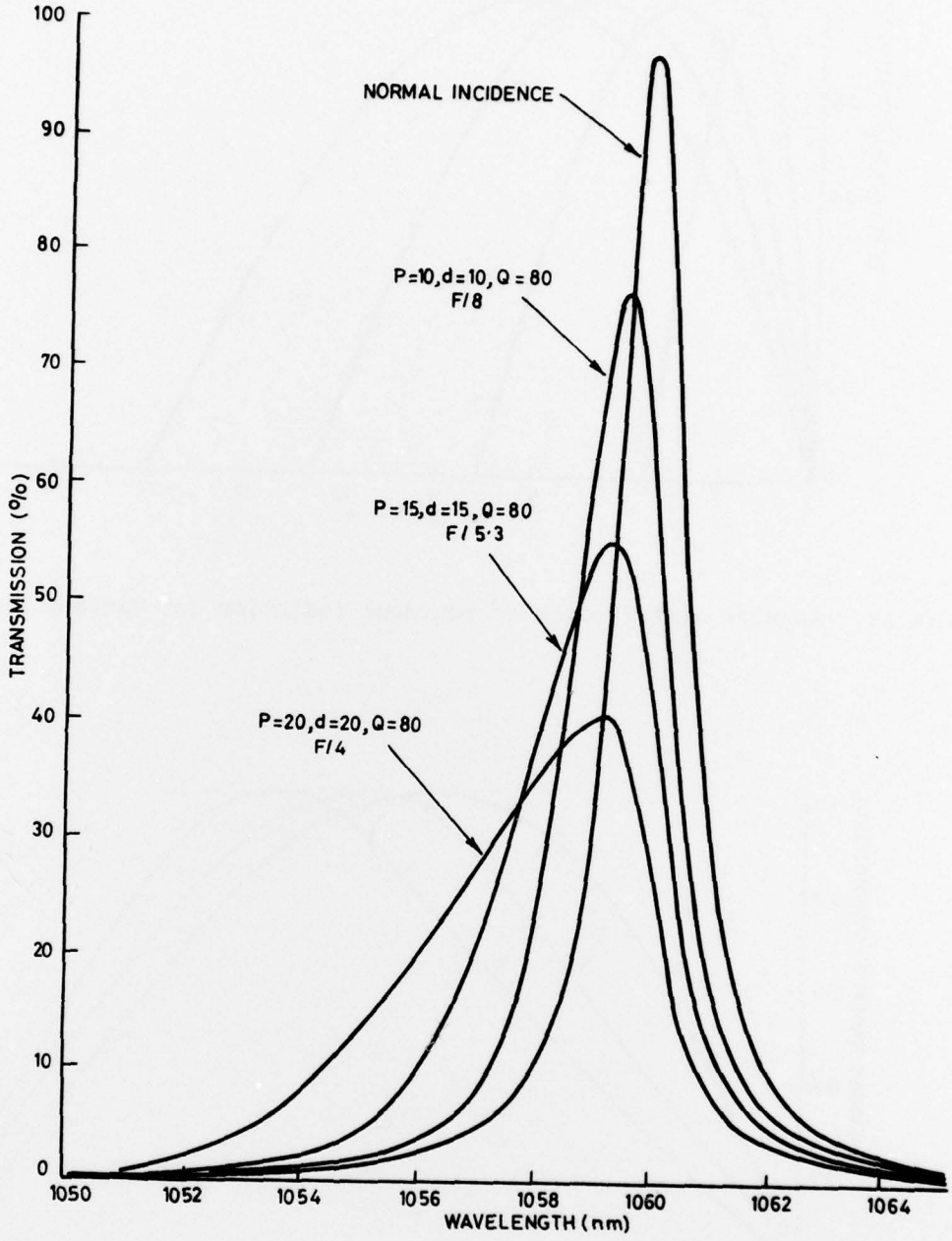

Figure 10. Filter performance changes due to variation in F number of optical system

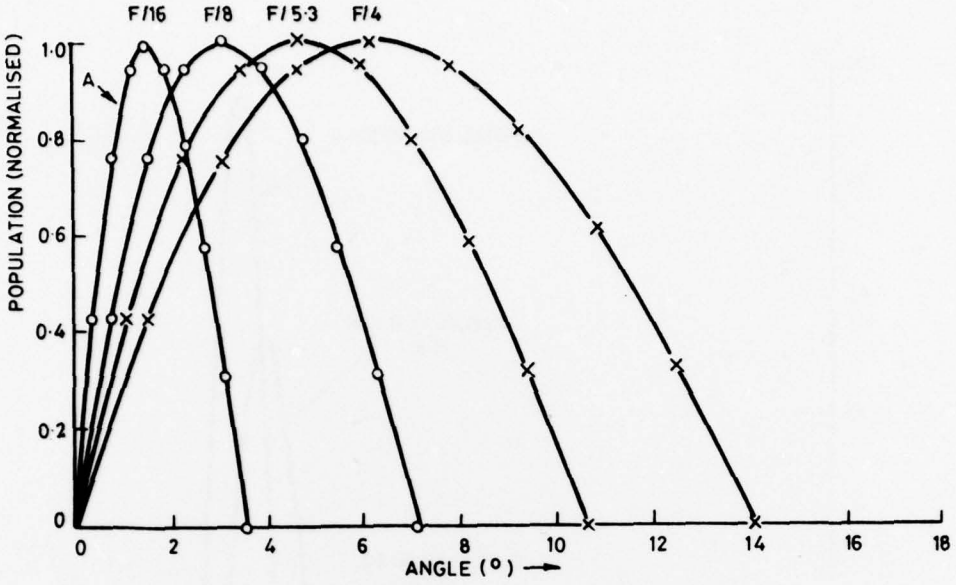

Figure 11. Angular distribution of incident radiation for various F numbers

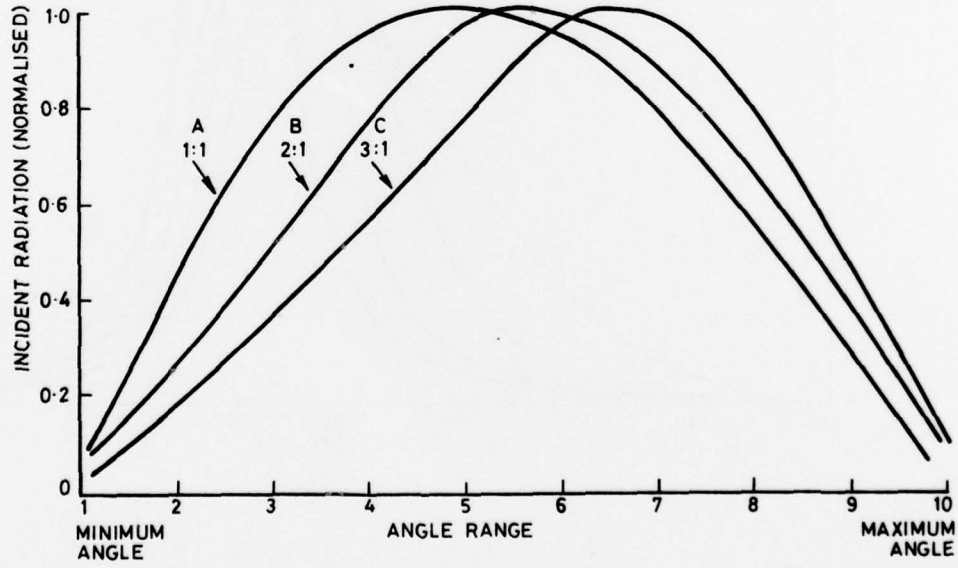

Figure 12. Angular distribution of incident radiation for various aperture/filter diameter ratios

DISTRIBUTION

EXTERNAL	Copy No.
In United States	
Counsellor, Defence Science, Washington	1
In United Kingdom	
Defence Scientific and Technical Representative, London	2
In Australia	
Chief Defence Scientist	3
Director, Joint Intelligence Organisation (DDSTI)	4
First Assistant Secretary, Computing Services	5
Executive Controller, Australian Defence Scientific Service	6
Superintendent, Defence Science Administration Division	7
Defence Information Services Branch (for microfilming)	8
Defence Library, Campbell Park	9
Library, Aeronautical Research Laboratories	10
Library, Materials Research Laboratories	11
Defence Information Services Branch for:	
United Kingdom, Ministry of Defence, Defence Research Information Centre (DRIC)	12
United States, Department of Defense, Defense Documentation Center	13 - 24
Canada, Department of National Defence, Defence Science Information Service	25
New Zealand, Department of Defence	26
Australian National Library	27
INTERNAL	
Director	28
Chief Superintendent, Applied Physics Wing	29
Chief Superintendent, Engineering Wing	30
Chief Superintendent, Weapons Research and Development Wing	31
Superintendent, Optics and Surveillance Division	32
Superintendent, Aerospace Division	33
Superintendent, Propulsion and Marine Physics Division	34
Superintendent, Communications and Electronic Engineering Division	35
Superintendent, Workshops and Mechanical Design Division	36
Principal Officer, Mechanical and Optical Techniques Group	37 - 38
Principal Officer, Laser Group	39
Principal Officer, Night Vision Group	40

	Copy No.
Principal Officer, Computing Services Group	41
Mr N.S. Bromilow, Mechanical and Optical Techniques Group	42
Mr H.J. Brophy, Mechanical and Optical Techniques Group	43
Mr M.W. Rossiter, Mechanical and Optical Techniques Group	44
Mr J.R. Venning, Mechanical and Optical Techniques Group	45
Mr R.J. Herbert, Mechanical and Optical Techniques Group	46
Mr D.E. Verringer, Mechanical and Optical Techniques Group	47
Mr M.R. Meharry, Night Vision Group	48
Mrs D. Williamson, Computing Services Group	49
Mr D.W. Faulkner, Laser Group	50
Mr K. Fueloep, Laser Group	51
Dr R.H. Hartley, Laser Group	52
Mr M.F. Penny, Laser Group	53
Dr D.M. Phillips, Laser Group	54
Mr D. Rees, Laser Group	55
Mr B.A. See, Laser Group	56
Author	57 - 61
W.R.E. Library	62 - 63
Spares	64 - 73